Ambiguity Functions of Laser-Based Chaotic Radar

Fan-Yi Lin and Jia-Ming Liu

***Abstract*—The ambiguity functions of a newly developed laser-based chaotic radar (CRADAR) system are studied. In the CRADAR system, the chaotic waveforms can be generated either by an optically injected (OI) semiconductor laser, or a semiconductor laser with optoelectronic feedback (OEF). The ambiguity functions of the chaotic pulsation and chaotic oscillation waveforms obtained experimentally from the CRADAR system with the respective OEF and the OI schemes are examined and compared. In the cross-ambiguity functions, both types of the chaotic waveforms demonstrate their excellent capabilities in the electrical counter-countermeasures (ECCM) that civilian and military applications desire. In the auto-ambiguity functions, the chaotic oscillation waveform shows better unambiguous detection quality than the chaotic pulsation waveform that an ideal thumbtack-like ambiguity function with minimal sidelobes is found. Moreover, variations in the peak value and the full width at half-maximum of the auto-ambiguity function of the chaotic oscillation waveform along the principal axes are also investigated. By having the features of both ultrawideband radar and random signal radar, the chaotic oscillation waveform of the CRADAR system with the OI scheme is shown to possess the advantages of high range resolution, excellent ECCM capability, ideal thumbtack-like ambiguity function, and uncoupled range and range rate resolution functions.**

***Index Terms*—Ambiguity function, chaos, radar, random signal radar, semiconductor lasers, ultrawideband.**

I. Introduction

ULTRAWIDEBAND (UWB) radars [1]–[4] and random signal radars (RSRs) [5]–[7] have been studied extensively in recent years. Compared with conventional radars, UWB radars possess the advantages of high range resolution, enhanced clutter-suppression capability, good penetration detection and imaging performances, narrowband radiation and noise immunity, and anti-jamming and counterstealth abilities. In contrast, RSRs have the advantages of low probability of intercept (LPI), excellent electrical counter-countermeasures (ECCM) performance, enhanced sea/ground clutter environment detection capability, and ideal thumbtack-like ambiguity function. Having the merits of both UWB radar and RSR, an UWB RSR [8] is highly desirable for both civilian and military applications that demand high-resolution target measurement and detection with diverse environmental adaptability.

A UWB random noise radar using a noise source has been developed and studied by Narayanan *et al.* [9]. Analyses in Doppler estimation [10], synthetic aperture radar (SAR) imaging [11], inverse SAR (ISAR) imaging [12], and ambiguity function characterization [13] have been reported. In this system and other RSR systems that generate random signals by amplifying thermal noise or utilizing electric circuits or devices [5], [9], [14], the bandwidths of the random signals are typically less than 1 GHz and the corresponding range resolutions are 15 cm or greater. With their noise-like property, possibilities of exploiting chaotic signals in radar systems have also been studied. Performance of a chaotic-signal frequency-modulation–continuous-wave (FM-CW) radar has been reported [15] and a chaotic signal radar system has been developed for vehicular collision-avoidance [16]. However, in both studies the chaotic signals are generated electronically, which have very limited bandwidths of 9.5 and 40 MHz, respectively.

To both improve the range resolution and further enhance the unique merits of UWB radars, a novel laser-based chaotic radar (CRADAR) system has been proposed and studied [17]. Instead of generating microwave noise or random signals by amplifying thermal noise or using electric circuits, the chaotic waveforms used in the CRADAR system are generated by semiconductor lasers based on nonlinear dynamics [18]. With proper setup and operating parameters, optically generated chaotic microwave waveforms can have bandwidths broader than 30 GHz [17], [19]. Although random signals with comparable bandwidths can certainly be generated by amplifying small-amplitude random sources such as thermal noise sources, it is difficult and costly to have comparable power because of the need of the broadband large-gain amplifiers. Contrarily, while the output power of semiconductor lasers can easily reach hundreds of milliwatts or even watts, the high cost in broadband amplification can be significantly reduced. Moreover, instead of using high-performance narrow-linewidth quality lasers used in optical communications, optical chaos can be generated with inexpensive ordinary semiconductor lasers.

Using laser dynamics as the source for radar system has another advantage over noise. By varying its operating condition, a laser can be easily switched among different dynamic states including periodic oscillation states, quasiperiodic pulsation states, regular pulsation states, chaotic pulsation states, and chaotic oscillation states [18]. These diverse waveforms with different characteristics are highly desirable for different applications. Moreover, unlike noise, optical chaotic signals with broad bandwidths can be sent to a distant radar platform through both free space or optical fiber with minimal attenuation and dispersion. This is especially important for the applications of bistatic or multistatic radars. Other advantages of using laser chaos also include the possibilities of synchronizing two or more radar systems [20], [21] and, with its coherent nature, using it as the source for arrayed radars.

By utilizing the ultrawideband noise-like chaotic waveforms, preliminary experiments in range finding employing the CRADAR system have been demonstrated [17]. The diverse waveforms generated by the CRADAR system have been

Manuscript received April 20, 2004; revised August 10, 2004.

The authors are with the Department of Electrical Engineering, University of California, Los Angeles, CA 90095-1594 USA (e-mail: liu@ee.ucla.edu).

Digital Object Identifier 10.1109/JQE.2004.836811

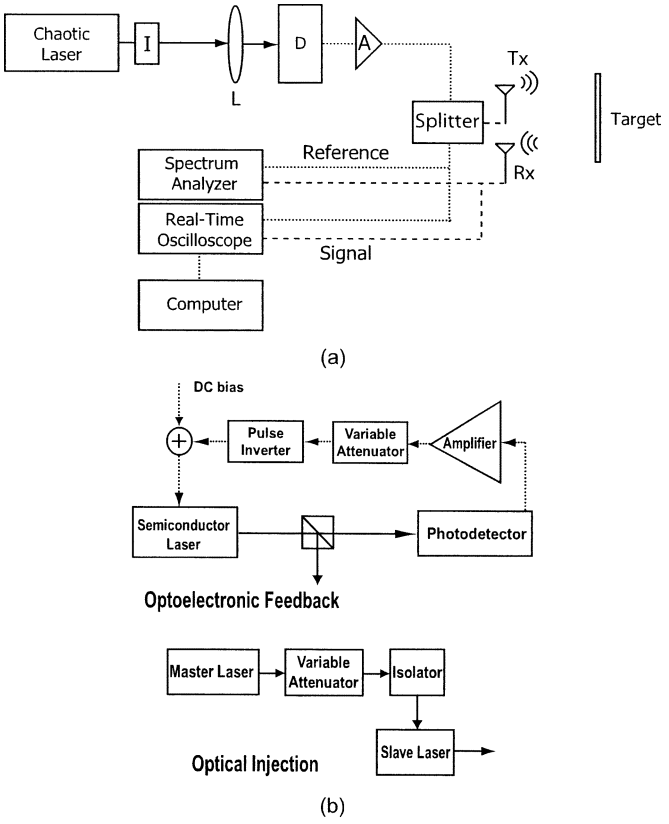

Fig. 1. (a) Schematic setup of the CRADAR system. I: isolator. L: lens. D: photodetector. A: amplifiers. Tx, Rx: transmitter and receiver antennas. (b) Block diagrams of the chaotic laser in an optoelectronic feedback scheme and an optical injection scheme. Dashed and solid lines indicate electronic and optic paths, respectively.

characterized [18]. Without down-converting the optical chaos to the microwave domain, a chaotic lidar (CLIDAR) system that probes and detects directly with the chaotic light has been proposed and studied as well [22].

Ambiguity functions best describe the detection property of a radar system in both the range and range rate domains [13], [23]. While ambiguity functions of chaotic phase modulated signals [24] and chaotic FM signals [25] generated with chaotic maps have been assessed for radar applications theoretically, the purpose of this paper is to study the ambiguity functions of the optically generated chaotic waveforms obtained experimentally from the CRADAR system. With two different perturbation schemes, namely, the optical injection (OI) and the optoelectronic feedback (OEF) schemes, two types of chaotic waveforms generated are considered and compared. Both auto- and cross-ambiguity functions of the optically generated chaotic waveforms are studied to understand the detection and the ECCM capabilities of the CRADAR system. The contours and the slices of the ambiguity functions along the principal axes are also investigated, and the potential applications of the CRADAR system are discussed as well.

II. CRADAR System Description

The schematic setup of the CRADAR system is shown in Fig. 1(a). Chaotic waveforms are generated by a semiconductor laser based on nonlinear dynamics. An optical isolator is placed after the laser to prevent unwanted optical feedback. The chaotic light is collected and detected by a combination of lens and detector. The microwave chaotic waveform is then amplified and split into two channels, the signal and the reference. The signal waveform is transmitted and received by a pair of antennas. Together with the reference waveform, these waveforms are recorded simultaneously with an RF spectrum analyzer and a real-time oscilloscope. Target detection and localization are accomplished through crosscorrelating the reference and the received signal waveforms. Signal processing and data analysis are performed in a personal computer. (Please see [15] for the detailed descriptions of the CRADAR system.)

In this paper, the ambiguity functions of the CRADAR system with two different schemes, the OEF and the OI schemes, are studied and compared. The block diagrams of the chaotic laser shown in Fig. 1(a) for these schemes are shown in Fig. 1(b). In the OEF scheme, the output of the semiconductor laser is either positively or negatively fed back to itself optoelectronically with a time delay [26], [27]. An InGaAsP–InP single-mode distributed feedback (DFB) laser with negative optoelectronic feedback is adopted in our experiment. The laser is biased at 35 mA and is stabilized at 21.0 °C for a resonance frequency of 1.5 GHz. A two-stage amplifier is used to amplify the feedback current, which is composed of two Avantek SSF886 amplifiers with a 3-dB passband of 0.4–3 GHz and a small-signal gain of about 60 dB. A Picosecond Pulse Lab Model 5100 broad-band pulse inverter is used to invert the electrical signal for negative feedback. The dynamics of the laser is controlled by adjusting the controllable operational parameters, which are the injection current, the feedback strength, and the delay time [26]. With proper adjustment, the semiconductor laser can be operated in a chaotic state that pulses irregularly [26]. In the OI scheme, a slave laser is optically injected by a master laser. The lasers used here are similar to the one used in the OEF scheme. The master and the slave lasers are biased at 59.89 and 50.00 mA and are stabilized at 13.0 °C and 23.0 °C, respectively. The detuning between the master and the slave lasers is around 2.7 GHz, and the free-running resonance frequency of the slave laser is 3 GHz. The dynamics of the slave laser is controlled by adjusting the controllable operational parameters, which are the injection current of the slave laser, the detuning frequency between the master and slave lasers, and the optical injection strength from the master to the slave laser [28]. With proper adjustment, the slave laser can be operated in a chaotic state that has a noise-like oscillation with a broad-band spectrum.

For both schemes, a high-speed InGaAs photodetector with a 6-GHz bandwidth is used to detect the chaotic waveforms. The chaotic waveforms are recorded on a Tektronix TDS694C digitizing real-time oscilloscope that has a 3-GHz bandwidth and a 10-GS/s sampling rate, and the corresponding power spectra are measured with an HP E4407B spectrum analyzer that has a 26.5-GHz bandwidth.

Fig. 2(a)–(c) and (d)–(f) shows the time series, the phase portraits, and the power spectra of the chaotic pulsation waveform and the chaotic oscillation waveform obtained with the OEF and the OI schemes, respectively. In the OEF scheme, the time series

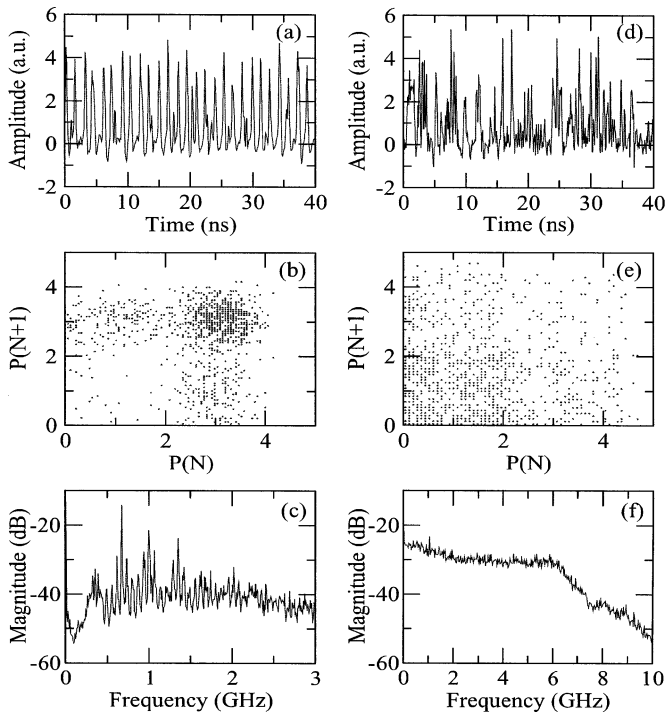

Fig. 2. Time series, phase portrait, and power spectrum of the chaotic states obtained experimentally for (a)–(c) the OEF scheme and (d)–(f) the OI scheme.

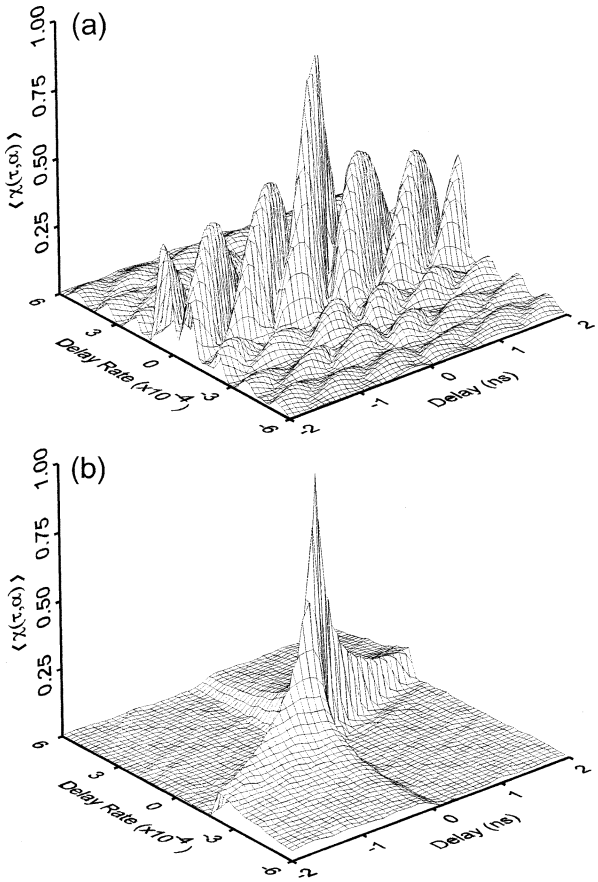

Fig. 3. Auto-ambiguity functions of the CRADAR system with (a) the OEF scheme and (b) the OI scheme. Correlation interval is $T = 10\ \mu$s.

in Fig. 2(a) shows a train of chaotic pulses, while the phase portrait in Fig. 2(b) that plots the correlation between consecutive peaks shows scattered dots with no discernible structure. With a main pulsation frequency at around 780 MHz, incommensurate frequencies can be found in the power spectrum shown in Fig. 2(c). In contrast, instead of chaotic pulses, chaotic oscillations with fine structures are found in the time series of the OI scheme shown in Fig. 2(d). Although the phase portrait in Fig. 2(e) also shows scattered dots without any distinguished pattern, the difference between the chaotic waveforms obtained with the OI and the OEF schemes are clearly demonstrated in their power spectra. Unlike the spiky spectrum seen in Fig. 2(c) for the chaotic pulsation waveform obtained with the OEF scheme, a rather flat and smooth spectrum that spans from dc to 6 GHz is found in Fig. 2(f) for the chaotic oscillation waveform obtained with the OI scheme. The drop seen at 6 GHz is due to the limited bandwidth of the detector used.

Noted that although these two distinct chaotic waveforms each represents the typical chaotic states observed in the respective OEF [26], [27] and OI schemes [29], both schemes can however produce both types of chaos under certain operating conditions [30]. While the detailed studies on the dynamics of these two schemes are reported elsewhere and are beyond the scope of this work, the emphasis of this paper will be on the characteristics of the ambiguity functions of these two different types of chaotic waveforms that are generally found in the respective OEF and OI schemes.

III. Ambiguity Function Analysis

In the CRADAR system, the chaotic waveforms are transmitted and received as baseband signals. Without a carrier that conventional radars typically have, the Doppler effect will cause only the compression or stretch of the transmitted waveforms depending on the target velocity. For a point target with a constant velocity v, the delay rate is $\alpha = 2v/(c-v) \simeq 2v/c$, where c is the speed of light. The ambiguity function is defined as

$$\langle \chi(\tau, \alpha, T) \rangle = \int_{t}^{t+T} u_{\mathrm{r}}(t) u_{\mathrm{s}}\left((1+\alpha)t - \tau\right) dt \qquad (1)$$

where u_{r} and u_{s} are the reference and the signal waveforms, τ is the relative delay time between the reference and the signal waveforms, and T is the correlation interval.

Fig. 3(a) and (b) shows the auto-ambiguity functions of the chaotic pulsation waveform and the chaotic oscillation waveform generated by the CRADAR system with the OEF and the OI schemes, respectively. These auto-ambiguity functions are obtained by autocorrelating the chaotic waveforms shown in Fig. 2(a) and (d) with a correlation interval of $T = 10\ \mu$s. As can be seen, the auto-ambiguity function of the chaotic pulsation waveform shown in Fig. 3(a) possesses many sidelobes that make unambiguous detection difficult. These sidelobes that deteriorate the detection performance are due to the repetitive pulses generated by the OEF scheme. In contrast, the auto-ambiguity function of the chaotic oscillation waveform shown in Fig. 3(b) possesses little to no sidelobe. Only a main peak is found in the center, indicating the excellent ability of the OI scheme in unambiguous detection. This ideal thumbtack-like

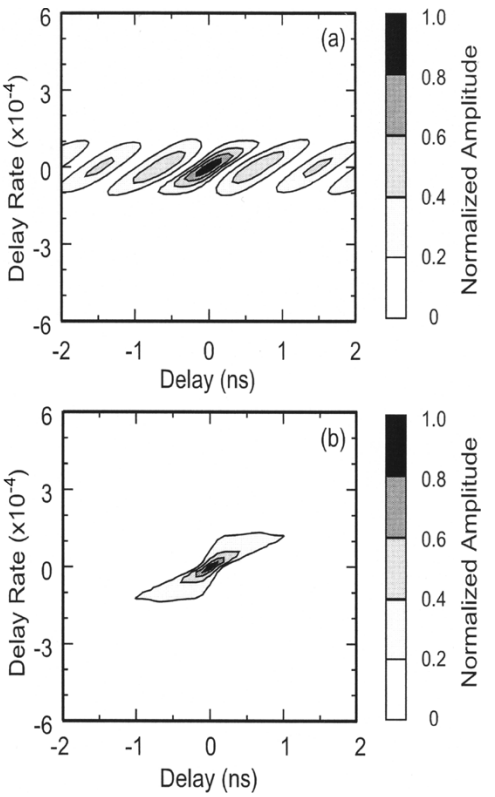

Fig. 4. Contours of the auto-ambiguity functions of the CRADAR system with (a) the OEF and (b) the OI schemes shown in Fig. 3(a) and (b), respectively.

ambiguity function results from the noise-like chaotic oscillation that has a flat and smooth spectrum with a very broad bandwidth. From the full-width at half maximum (FWHM) of the peak in the delay and delay rate axes, range and range rate resolutions of 3 cm and 7 km/s, respectively, are derived. While a 7-km/s range rate resolution seems not practical, it is worth mentioning that the range and range rate resolutions of the CRADAR system are currently limited not by the chaotic waveforms, but are respectively limited by the available detection bandwidth of the real-time oscilloscope used and the 10-μs correlation interval. Noted that the 10-μs correlation interval is chosen so that the details of the range rate function and its relation with the delay, the delay rate, and the correlation interval can be clearly shown. Nevertheless, since the range and the range rate resolution functions are uncoupled due to the correlation process [13], the range rate resolution of the CRADAR system can be improved to a practical range by simply increasing the correlation interval without compromising the outstanding range resolution. For instance, with a correlation interval of 100 ms, an estimated range rate resolution of 0.7 m/s can be achieved.

Fig. 4(a) and (b) shows the contours of the auto-ambiguity functions shown in Fig. 3(a) and (b), respectively. The values of the ambiguity functions are represented by the gradients with an interval of 0.2. As can be seen, while many islands are found along the zero delay rate axis in the contour of the chaotic pulsation waveform shown in Fig. 4(a), only a single island is found in the center of the contour of the chaotic oscillation waveform shown in Fig. 4(b) implying a better unambiguous detection performance. Note that the islands in both plots are skewed

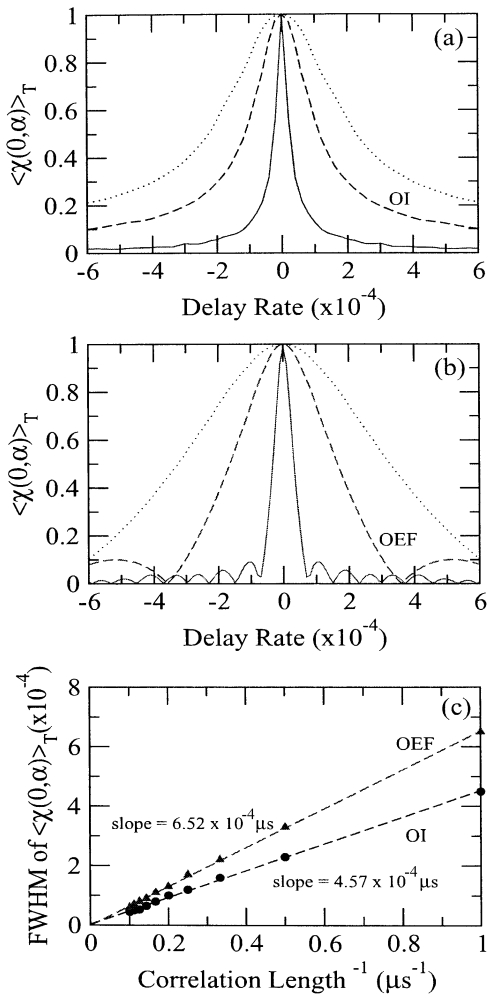

Fig. 5. Slices of $\langle\chi(0,\alpha)\rangle_T$ for different values of correlation interval T of the (a) OI and (b) OEF schemes, respectively. (c) Full-width at half maximum of $\langle\chi(0,\alpha)\rangle_T$ versus T, where the dashed lines are linear regressions.

along the same direction. Unlike the ridges seen in linear frequency modulated and stepped frequency radar systems which are due to the coupling between the Doppler frequency shift and the modulation frequency generated, the skewness in this baseband CRADAR system is caused by the coupling between the delay time τ and the delay rate α as indicated in (1). With this skewed nature, the chaotic oscillation waveform obtained with the OI scheme is found to have a slightly better unambiguous detection performance in the second and fourth quadrants of the delay-delay rate plane than in the first and third quadrants.

To investigate the relation between the correlation interval and the ambiguity function, slices of $\langle\chi(0,\alpha)\rangle_T$ at zero delay for different values of correlation interval T are plotted and compared for the chaotic waveforms. Fig. 5(a) and (b) shows the slices of $\langle\chi(0,\alpha)\rangle_T$ for the chaotic pulsation and chaotic oscillation waveforms with $T = 1$, 2, and 10 μs in the dotted, dashed, and solid curves, respectively. As can be seen in both Fig. 5(a) and (b), the widths of the slices narrow when the correlation interval increases. The FWHM of the slices of the chaotic pulsation and chaotic oscillation waveforms are plotted with triangles and circles in Fig. 5(c), respectively, to the inverse of the correlation interval. The dashed lines are the linear regressions.

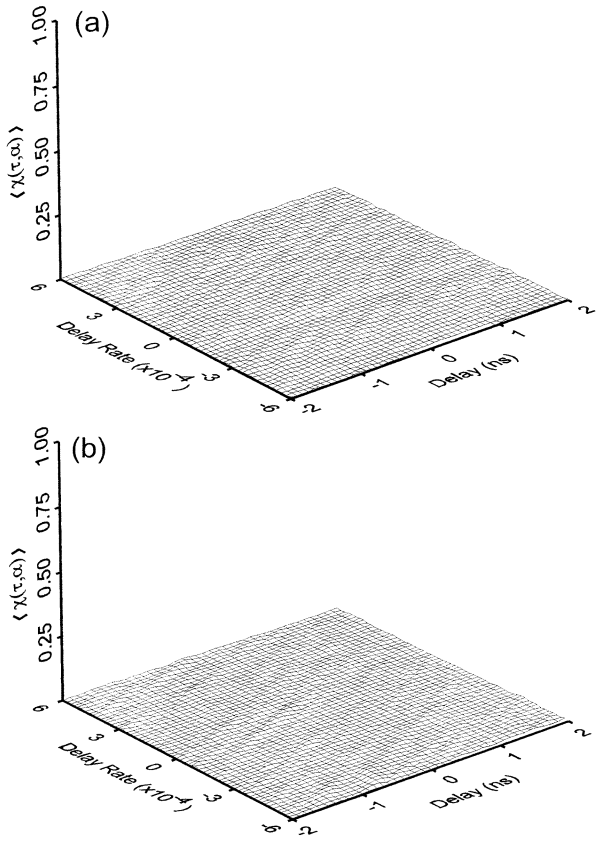

Fig. 6. Cross-ambiguity functions of the CRADAR system with (a) the OEF scheme and (b) the OI scheme. Correlation interval is $T = 10\ \mu$s.

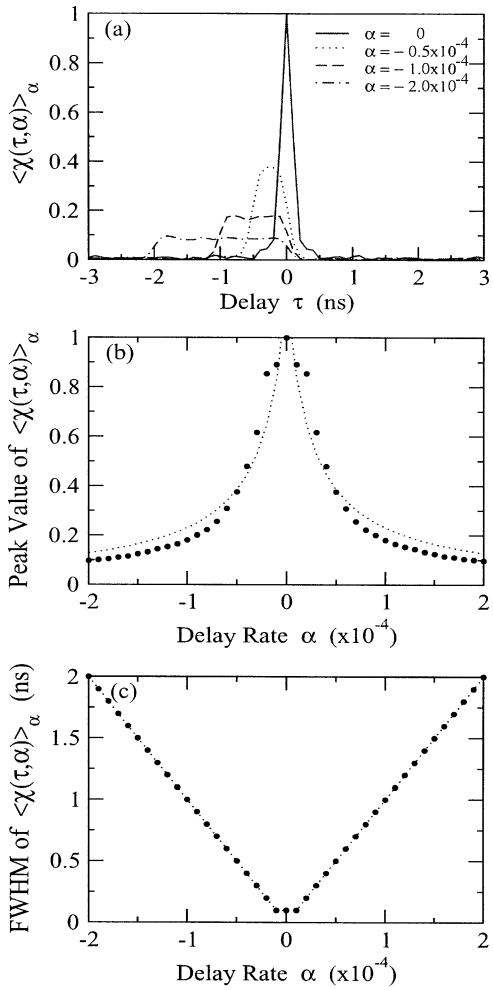

Fig. 7. (a) Slices of $\langle\chi(\tau,\alpha)\rangle_\alpha$ for different α with the correlation interval $T = 10\ \mu$s. (b) Peak value and (c) full-width at half maximum of $\langle\chi(\tau,\alpha)\rangle_\alpha$ for different α, where the dotted curves and lines are, respectively, inverse and linear fittings.

As can be seen, the FWHM of the slices for both waveforms are inversely proportional to the correlation interval. In other words, the range rate resolution can be improved linearly with the correlation interval, or the bandwidth of the correlation process. Note that with the same correlation interval, the range rate resolution of the chaotic oscillation waveform is found to be slightly better than the chaotic pulsation waveform as indicated by the slopes of the regressions shown in Fig. 5(c).

Besides unambiguous detection, another very important performance factor in modern radar systems is the ECCM capability. Unlike the white noise, chaotic signals are not necessarily uncorrelated with each other for a given time interval. In fact, it is strongly dependent on its complexity and predictability governed mainly by the largest positive Lyapunov exponent [22]. Therefore, to inspect the ECCM capability and the quality of the interference immunity of the CRADAR system, Fig. 6(a) and (b) plots the cross-ambiguity functions of the chaotic waveforms obtained with the OEF and the OI schemes, respectively. These cross-ambiguity functions are obtained by crosscorrelating the chaotic waveforms shown in Fig. 2(a) and (d) with the waveforms obtained under the same operation conditions but at a different time with a correlation interval of $T = 10\ \mu$s, which simulates the situation that the CRADAR system is interfered with another similar radar system. As can be seen in Fig. 6(a) and (b), only mild ripples are presented on the surfaces with no discernible spikes. These ideal cross-ambiguity functions reflect the non repetitive random nature of the chaotic waveforms. Unlike man-made random or chaotic codes, which are pseudorandom at best, chaotic waveforms generated by the nonlinear dynamics of lasers at different times are not repetitive and are barely correlated with each other. Accordingly, the CRADAR system with either scheme has a very good performance in the ECCM capability, which is critical particularly in the short range, multi-user, and arrayed radar applications.

By featuring the complex chaotic oscillation waveform that has a broad, flat, and smooth spectrum, the CRADAR system with the OI scheme is shown to be the better scheme that has not only an excellent ECCM capability but also great performances in unambiguous detections compared to the OEF scheme. To further examine the auto-ambiguity function of the chaotic oscillation waveform obtained with the OI scheme, the slices of $\langle\chi(\tau,\alpha)\rangle$ in the principal axes are plotted in Figs. 7 and 8.

Fig. 7(a) shows the slices of $\langle\chi(\tau,\alpha)\rangle_\alpha$ for different values of α. It is seen that as $|\alpha|$ increases, the peak value of the slice decreases and the width increases. The relation between α and the peak value and that between α and the FWHM of the peak are shown in Fig. 7(b) and (c), respectively. The dotted curves in Fig. 7(b) are inverse fittings, and the lines in Fig. 7(c) are linear fittings. As can be seen, the value of the correlation peak

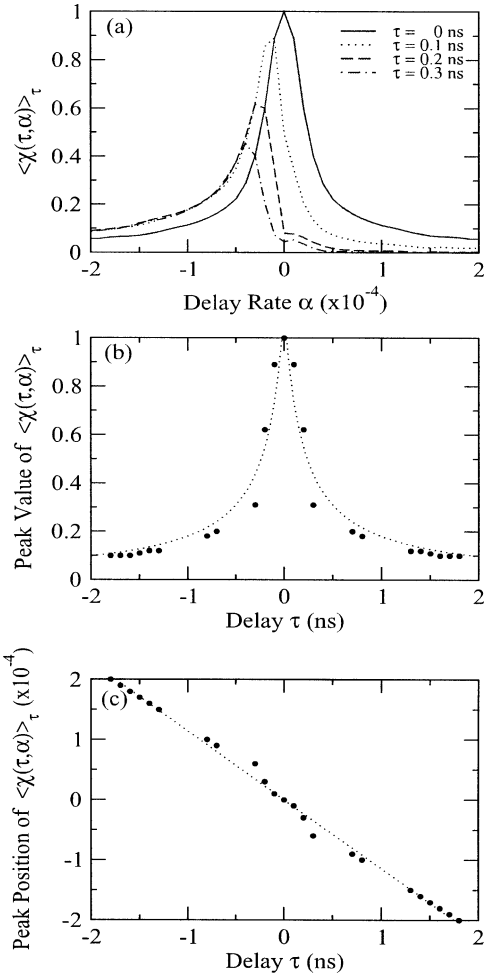

Fig. 8. (a) Slices of $\langle \chi(\tau, \alpha) \rangle_\tau$ for different τ with the correlation interval $T = 10\ \mu$s. (b) Peak value and (c) relative position of the peak of $\langle \chi(\tau, \alpha) \rangle_\tau$ for different τ, where the dotted curves and line are, respectively, inverse and linear fittings.

decreases inversely with $|\alpha|$ while the FWHM of the peak increases linearly. These are the consequence of Doppler compression and broadening in the spectrum of the received waveform. For a baseband signal with an evenly distributed power spectral density such as the one obtained from the OI scheme, the Doppler effect causes the effective bandwidth of the return signal to vary with α linearly.

Fig. 8(a) shows the slices of $\langle \chi(\tau, \alpha) \rangle_\tau$ for different values of τ. It is seen that as $|\tau|$ increases, the peak value of the slice decreases and the position of the peak shifts away from the zero delay rate. The relation between τ and the peak value and that between τ and the peak position are shown in Fig. 8(b) and (c), respectively. The dotted curves in Fig. 8(b) are inverse fittings, and the line in Fig. 8(c) is linear fitting. As can be seen, the value of the correlation peak decreases inversely with $|\tau|$ while the shift in the peak position increases linearly.

IV. Discussion and Conclusion

The ambiguity functions of two distinct chaotic waveforms, namely the chaotic pulsation and the chaotic oscillation waveforms, generated by the laser based CRADAR system with the respective OEF and the OI schemes are studied and compared. Benefited from the complexity and unpredictability, both types of chaotic waveforms generated by the nonlinear laser dynamics show excellent ECCM capabilities that surfaces with only mild ripples are seen in the cross-ambiguity functions. While many sidelobes are found in the auto-ambiguity function of the chaotic pulsation waveform that deteriorates its unambiguous detection performance, the auto-ambiguity function of the chaotic oscillation waveform is an ideal thumbtack-like function that has a single peak in the center without any discernible sidelobes. The slices of the auto-ambiguity function of the chaotic oscillation waveform along the principal axes are also examined. It is found that the value of the peak varies with both $|\alpha|$ and $|\tau|$ inversely, while the FWHM of the peak and the shift in peak position vary with both $|\alpha|$ and $|\tau|$ linearly.

As shown in this paper, by adopting the chaotic oscillation waveform produced by the OI scheme that has a flat, smooth, and broad spectrum, the CRADAR system can have the advantages of both an UWB radar and a random signal radar that has excellent ECCM performance, unambiguous detection capability, and outstanding range resolution. A 3-cm-range resolution deriving from the FWHM of the auto-ambiguity function is achieved experimentally, which is currently limited not by the bandwidth of the chaotic oscillation waveform but by the detection bandwidth of the real-time oscilloscope used. With this already superb range resolution, the CRADAR system is surely desired for applications such as traffic guiding and collision avoidance, infrastructure integrity assessment, microwave imaging, through-wall detection, and object tracking and locating.

References

[1] G. Liu, H. Gu, X. Zhu, and W. Su, "The present and the future of random signal radars," *IEEE Aerosp. Electron. Syst. Mag.*, vol. 12, pp. 35–40, Oct. 1997.

[2] I. I. Immoreev and D. V. Fedotov, "Ultrawideband radar systems: advantages and disadvantages," in *Proc. IEEE Conf. Ultra Wideband Syst. and Tech.*, Picataway, NJ, 2002, pp. 201–205.

[3] J. D. Taylor, *Ultra-Wideband Radar Technology*. New York: CRC, 2001.

[4] F. Chevalier, "Future concepts for electromagnetic detection: from space-time-frequency resources management to wideband radars," *IEEE Aerosp. Electron. Syst. Mag..*, vol. 14, pp. 9–17, Oct. 1999.

[5] M. I. Sobhy and A. R. Shehata, "Chaotic radar systems," in *Proc. IEEE MTT-S Int. Microwave Symp. Dig.*, vol. 3, Piscataway, NJ, 2000, pp. 1701–1704.

[6] G. Liu, H. Gu, and W. Su, "Development of random signal radars," *IEEE Trans. Aerosp. Electron. Syst.*, vol. 35, pp. 770–777, July 1999.

[7] G. Liu, H. Gu, W. Su, H. B. Sun, and J. H. Zhang, "Random signal radar—a winner in both the military and civilian operating environments," *IEEE Trans. Aerosp. Electron. Syst.*, vol. 39, pp. 489–498, Apr. 2003.

[8] H. Sun, Y. Lu, and G. Liur, "Ultra-wideband technology and random signal radar: an ideal combination," *IEEE Aerosp. Electron. Syst. Mag.*, vol. 18, pp. 3–7, Nov. 2003.

[9] R. M. Narayanan, Y. Xu, P. D. Hoffmeyer, and J. O. Curtis, "Design, performance, and applications of a coherent ultra-wideband random noise radar," *Opt. Eng.*, vol. 37, no. 6, pp. 1855–1869, Jun. 1998.

[10] R. M. Narayanan and M. Dawood, "Doppler estimation using a coherent ultrawide-band random noise radar," *IEEE Trans. Antennas Propagat.*, vol. 48, pp. 868–878, June 2000.

[11] D. S. Garmatyuk and R. M. Narayanan, "Ultra-wideband continuous-wave random noise arc-SAR," *IEEE Trans. Geosci. Remote Sensing*, vol. 40, pp. 2543–2552, Dec. 2002.

[12] D. C. Bell and R. M. Narayanan, "ISAR imaging using a coherent ultra-wideband random noise radar system," *Opt. Eng.*, vol. 40, no. 11, pp. 2612–2622, Nov. 2001.

[13] M. Dawood and R. M. Narayanan, "Generalized wideband ambiguity function of a coherent ultrawideband random noise radar," *Proc. Inst. Elect. Eng., Radar Sonar Navig.*, vol. 150, no. 5, pp. 379–386, 2003.
[14] Y. Shen and G. Liu, "Use chaos to generate broadband signals," *Proc. SPIE*, vol. 3702, pp. 144–151, 1999.
[15] W. Machowksi and P. Ratliff, "Performance indications of a novel chaotic-signal FM-CW radar for multi-user applications," in *Proc. Radar Conf.*, Edinburgh, U.K., Oct. 2002, pp. 474–477.
[16] Y. Hara, T. Hara, T. Seo, H. Yanagisawa, P. Ratliff, and W. Machowksi, "Development of a chaotic signal radar system for vehicular collision-avoidance," in *Proc. Radar Conf.*, Edinburgh, U.K., Oct. 2002, pp. 227–232.
[17] F. Y. Lin and J. M. Liu, "Chaotic radar using nonlinear laser dynamics," *IEEE J. Quantum Electron.*, vol. 40, pp. 815–820, June 2004.
[18] ——, "Diverse waveform generation using semiconductor lasers for radar and microwave applications," *IEEE J. Quantum Electron.*, vol. 40, pp. 682–689, June 2004.
[19] ——, "Nonlinear dynamical characteristics of an optically injected semiconductor laser subject to optoelectronic feedback," *Opt. Commun.*, vol. 221, no. 1–3, pp. 173–180, 2003.
[20] M. Bucolo, R. Caponetto, L. Fortuna, M. Frasca, and A. Rizzo, "Does chaos work better than noise?," *IEEE Circuits Syst. Mag.*, vol. 2, pp. 4–19, Third Quarter 2002.
[21] S. Tang and J. M. Liu, "Chaos synchronization in semiconductor lasers with optoelectronic feedback," IEEE J. Sect. Topics Quantum Electron., vol. 39, pp. 708–715, June 2003, to be published.
[22] F. Y. Lin and J. M. Liu, "Chaotic lidar," IEEE J. Quantum Electron., to be published.
[23] L. O'Carroll, D. H. Davies, C. J. Smyth, J. H. Dripps, and P. M. Grant, "A study of auto- and cross-ambiguity surface performance for discretely coded waveforms," *Proc. Inst. Elect. Eng.*, vol. 137, no. 5, pp. 362–370, 1990.
[24] Y. Shen, W. Shang, and G. Liu, "Ambiguity function of chaotic phase modulated radar signals," in *Proc. 4th Int. Conf. Signal Processing*, vol. 2, Beijing, China, Oct. 1998, pp. 1574–1577.
[25] B. C. Flores, E. A. Solis, and G. Thomas, "Assessment of chaos-based FM signals for range-Doppler imaging," *Proc. Inst. Elect. Eng., Radar Sonar Navig.*, vol. 150, no. 4, pp. 313–322, Aug. 2003.
[26] F. Y. Lin and J. M. Liu, "Nonlinear dynamics of a semiconductor laser with delayed negative optoelectronic feedback," *IEEE J. Quantum Electron.*, vol. 39, no. 4, pp. 562–568, Apr. 2003.
[27] S. Tang and J. M. Liu, "Chaotic pulsing and quasiperiodic route to chaos in a semiconductor laser with delayed opto-electronic feedback," *IEEE J. Quantum Electron*, vol. 37, pp. 329–336, Mar. 2001.
[28] T. B. Simpson, J. M. Liu, K. F. Huang, and K. Tai, "Nonlinear dynamics induced by external optical injection in semiconductor lasers," *Quantum Semiclass. Opt.*, vol. 9, pp. 765–784, Oct. 1997.
[29] T. B. Simpson, J. M. Liu, A. Gavrielides, V. Kovanis, and P. M. Alsing, "Period-doubling cascades and chaos in a semiconductor laser with optical injection," *Phys. Rev. A*, vol. 51, pp. 4181–4185, May 1995.
[30] S. Wieczorek, T. B. Simpson, B. Krauskopf, and D. Lenstra, "Bifurcation transitions in an optically injected diode laser: theory and experiment," *Opt. Commun.*, vol. 215, no. 1–3, pp. 125–134, Jan. 2003.

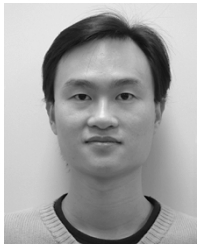

Fan-Yi Lin was born in Hsinchu, Taiwan, R.O.C., in 1975. He received the B.S. degree in electrophysics from National Chiao-Tung University, Hsinchu, Taiwan, R.O.C., in 1997 and the M.S. and Ph.D. degrees in electrical engineering from the University of California, Los Angeles, in 2001 and 2004, respectively.

He is currently an Assistant Professor with the Department of Electrical Engineering and Institute of Photonics Technologies, National Tsinghua University, Hsinchu. His current research interests include nonlinear laser dynamics, optoelectronics, and lidar and radar systems.

Jia-Ming Liu was born in Taiwan, R.O.C., on July 13, 1953. He received the B.S. degree in electrophysics from National Chiao-Tung University, Taiwan, R.O.C., in 1975, and the S.M. and Ph.D. degrees in applied physics from Harvard University, Cambridge, MA, in 1979 and 1982, respectively.

He was an Assistant Professor with the Department of Electrical and Computer Engineering, State University of New York at Buffalo, Amherst, from 1982 to 1983 and was a Senior Member of the Technical Staff with GTE Laboratories, Inc., from 1983 to 1986. He is currently a Professor with the Electrical Engineering Department, University of California, Los Angeles. His research interests include development and application of picosecond and femtosecond wavelength-tunable infrared laser pulses, nonlinear and dynamic processes in semiconductor materials and lasers, wave propagation in optical structures, and chaotic synchronization in optical systems.

Dr. Liu is a Fellow of the Optical Society of America, a Senior Member of the IEEE Laser and Electro-Optics Society, and a member of the American Physical Society, the Phi Tau Scholastic Honor Society, and Sigma Xi. He is also a founding member of the Photonics Society of Chinese-Americans. He became a licensed professional electrical engineer in 1977.